International Journal of Environment and Pollution Research
Vol.6, No.3, pp.39-51, August 2018
Published by European Centre for Research Training and Development UK (www.eajournals.org)

DOES AIR-SEA COUPLING IMPROVE TROPOSPHERIC OZONE SIMULATION?

Hyo-Jin Park[1,2], Byung-Kwon Moon[2], Jieun Wie[2]

[1]Gunsan Dongsan Middle School, Gunsan 54020, South Korea
[2]Division of Science Education / Institute of Fusion Science, Chonbuk National University, Jeonju 54896, South Korea

ABSTRACT: *Air-sea coupling has a significant impact on monsoon circulation and precipitation distribution in East Asia during summer. Despite this, its impact on tropospheric ozone simulations has not been extensively researched. We ran the global chemistry transport model using the meteorological data obtained from the coupled general circulation model and the atmospheric circulation model, and analysed the characteristics of the simulations with respect to the distribution of tropospheric ozone over East Asia with and without consideration of the air-sea interaction. When the air-sea interaction was considered, the average concentration of ozone simulated for East Asia in August–September was closer to observation than when the interaction was not considered. This result can be attributed to the improvement in simulating the monsoon circulation and precipitation distribution. The air-sea coupling was also essential in simulating the relationship between the Western North Pacific Subtropical High and East Asian ozone, although there were some errors in the distribution and magnitude of ozone variability. In addition, the model simulations show that the ozone response due to the strengthened monsoonal front is inclined northward in altitude, which calls for further observational evidence.*

KEYWORDS: Air-Sea Interaction, Tropospheric Ozone, Chemistry Transport Model, Western North Pacific Subtropical High

INTRODUCTION

Tropospheric ozone is a pollutant that causes premature mortality in humans (Jerrett et al. 2009; Lelieveld et al. 2015), as well as greenhouse gas prompted climate warming (Shindell et al. 2006). Ozone is also responsible for a decline in grain production as it has a negative influence on plant growth (Burney,Ramanathan 2014). The increase in ground-level ozone concentrations being observed in East Asia over the last several decades is mainly due to an increase of precursor emissions (Wang et al. 2009; Tanimoto et al. 2009). A chemical transport model to simulate ozone is expected to play an important role in managing the air quality and establishing climate change adaptation policies. However, the model simulations are still quite different from observations (Han et al. 2008). Lin et al. (2009) pointed out the necessity of resolving emissions uncertainties, implementing a more precise chemical process, and improving the model resolution in order to obtain more realistic simulations.

Here, we focused on the fact that meteorological variables are also critical factors in determining ozone concentration (Chatani,Sudo 2011; Kurokawa et al. 2009). In East Asia, surface ozone concentrations are lower in summer than they are in autumn and spring, contrary to the summertime maximum in North America and Europe (Parrish et al. 2013). This is due to the effect of the East Asian summer monsoon (EASM) that results from sea-land thermal differences (He et al. 2008; Lin et al. 2009). The reliability of the simulations of the monsoon cloud band and precipitation needs to be ascertained in order to achieve a precise simulation of

ISSN: 2056-7537(print), ISSN 2056-7545(online)

the tropospheric ozone (Chatani,Sudo 2011). However, the characteristics of the EASM simulated by climate models are far from realistic (Huang et al. 2013). Most climate models can neither accurately locate the monsoonal precipitation band, nor can they simulate the amount of precipitation.

Note that models that include air-sea interaction, as opposed to those that do not, yield more realistic simulations of the precipitation distribution related to the EASM and low-level winds (Wang et al. 2005; Song,Zhou 2014). Considering the above-mentioned impact of the summer monsoon on tropospheric ozone, a better representation of EASM with an air-sea coupled model may improve simulations of tropospheric ozone in chemical transport models. However, the effect of including air-sea interaction in East Asian ozone simulations with atmospheric chemistry models has not been studies. In this study, we attempt to confirm the hypothesis that the performance of East Asian ozone simulations can be improved when meteorological variables inherent to air-sea coupling processes are used to drive a global chemistry transport model. Due to a lack of ground-based ozone observations in East Asia, we focused on the tropospheric column ozone which is available freely from satellite observation.

Model experiments and observation data

A global 3-D chemical transport model (GEOS-Chem) was used to simulate the tropospheric ozone concentration over East Asia. The Geos-Chem was originally developed to be driven by the meteorological fields from the Goddard Earth Observing System (GEOS) of the NASA Global Modelling and Assimilation Office (Bey et al. 2001; Park et al. 2004). We use the GEOS-Chem version 8-01-03 global 3-D model with 2˚×2.5˚ horizontal resolution (http://wiki.seas.harvard.edu/geos-chem/index.php/GEOS-Chem_v8-01-03). Instead of using GEOS input, the GEOS-Chem code was slightly modified to utilize the meteorological data from the Community Climate System Model version 3 (CCSM3) (Collins et al., 2006a).

In order to prepare the meteorological data for GEOS-Chem, we conducted two runs with CCSM3. We started with a fully coupled component set-up that included atmosphere (CAM3), land (CLM3), and the ocean and sea ice models called POP and CSIM, respectively, mutually linked by means of a coupler. The atmospheric model had a finite volume dynamic core with a 2˚×2.5˚ horizontal grid and 26 vertical levels. The land component had the same horizontal resolution as the atmospheric model. The ocean and ice models shared an identical horizontal grid (gx1v3) with the North Pole displaced into Greenland. In the ocean model, there were 40 vertical levels with thicknesses monotonically increasing from approximately 10 to 250 m. A more detailed description of the CCSM3 can be found in a previous study by Collins et al. (2006a). This coupled climate model was run for 280 years and its latest 45-year simulated meteorological fields were used to drive the GEOS-Chem. We refer to this GEOS-Chem simulation for 45 years as the CChem run.

Another experiment (AChem run), similar to CChem run, except in the CCSM3 component had only two components; atmosphere (CAM3) and land model (CLM3), that were activated to simulate meteorological variables. Thus, the CCSM3 needed to be forced with the observed sea surface temperature (SST) and sea ice concentration. In this case CCSM3 run was performed for the period from 1960 to 2010 with the Hadley Centre Sea Ice and SST dataset (HadISST), producing meteorological data for GEOS-Chem, after which GEOS-Chem was carried out with the CCSM3 output during the last 40 years (1971–2010). Here, in the both CChem and AChem runs, biomass and anthropogenic emission are seasonal but are annually invariant. Hence, our simulation does not specifically include the interannual variations of

ISSN: 2056-7537(print), ISSN 2056-7545(online)

biomass burning emission. Specifically, any modeled correlations in this study cannot be due to the emission. The initial conditions for AChem and CChem are from a previous multiyear GEOS-Chem run that was forced with the CCSM3 simulations using climatological SSTs. Both experiments are summarized in Table 1.

The gridded tropospheric ozone data based on the Aura Ozone Monitoring Instrument (OMI) and Microwave Limb Sounder (MLS) (Ziemke et al. 2006; Ziemke et al. 2011), the NCEP reanalysis-2 data, and the CMAP precipitation for the period 2005 to 2014 are compared with our simulations.

Impact of air-sea coupling on climatological ozone

Figure 1a shows the average tropospheric ozone distributions obtained from the two model simulations and observations. The observed ozone concentrations are low in the tropical Western Pacific and high in East Asia (the area marked as a green rectangle); this contrast is evident in the two models. Minimum ozone concentrations are evident in the tropical Western Pacific because of the high convective activity in this area (Doherty et al. 2005). While observations in East Asia present a large ozone concentration in the northeast-southwest direction, both models yield zonally elongated ozone. These common biases in simulated ozone imply that the meteorological fields used in CChem and AChem have similar errors, which are probably rooted in the same atmospheric model (see Song,Zhou 2014).

The averaged ozone concentration of AChem for East Asia is higher than that of CChem. Such a difference is prominent in August, September, October, and November (Fig. 1b). In particular, the ozone concentrations of observation and CChem run are shown to be quite similar in August–September, not only with regard to mean ozone but also to the interquartile range, which is statistically significant at the 99% confidence level. However, ozone concentrations were highest in August–September in AChem run, presenting a large difference from CChem run. The ozone differences between CChem run and AChem run were concentrated in the EASM region (Fig. 1c). Compared to CChem run, AChem run overestimates the concentration of ozone in Eastern China, the Korean Peninsula, and Japan. Lin et al. (2009) suggested that the over-estimation of ozone concentrations in East Asia resulted from the under-estimation of monsoon precipitation and cloud cover by atmospheric models. It is thus necessary to evaluate whether the anomalous ozone in AChem run is related to meteorological fields containing more biases than CChem run due to the lack of air-sea interactions.

Fig. 2a–c shows the average precipitation and 850hPa wind from observation and simulations during August–September. In this period, observations are dominated by the band of precipitation that stretches from the tropics to the Korean Peninsula and Japan, along with the southwesterly wind that blows from the Western North Pacific. Both models cannot reproduce this band of precipitation well, and both show heavy precipitation over Western China, probably caused by the strong easterly wind. However, it is evident that the precipitation and wind simulated by CChem run resembles the observation more closely than the AChem run. The difference between the two models is shown in Fig 2d, where the precipitation of CChem run is heavier than AChem run across mid-China, the Korean Peninsula, and Japan, and simultaneously, along with the monsoon-like anticyclonic circulation, precipitation in southern China and Southeastern Japan is lower. It can be said that the atmospheric field produced by CChem run reproduces monsoon circulation more realistically than AChem run. These differences between CChem run and AChem run are similar to discrepancies in precipitation

ISSN: 2056-7537(print), ISSN 2056-7545(online)

and wind fields analyzed using the 17 air-sea coupled models and atmospheric models (see Fig. 2c from Song,Zhou (2014)).

Note that different patterns in the tropospheric ozone (Fig. 1c) and precipitation (Fig. 2d) show a negative relationship between the two variables, implying that the difference of tropospheric ozone between CChem run and AChem run (Fig. 1c) is mainly due to the different meteorological data used in the two experiments. This is basically understood to be a consequence of whether the air-sea coupling process was included or not. These results show that for East Asian ozone simulations, meteorological data that incorporate the air-sea interaction must be used.

Song,Zhou (2014) suggest that coupled models simulate the East Asian summer monsoon better than atmospheric models because the Western North Pacific sea surface temperature (SST) of the coupled models is lower than that of observations. The low SST leads to a decrease in evaporation and precipitation, and this ultimately strengthens the subtropical anticyclone of the Western North Pacific and monsoon circulation. In order to verify if this is relevant to our simulations, the differences in the 850 hPa geopotential height and sea surface temperature (SST) between the two models (CChem minus AChem) were analyzed (Fig. 2e, 2f). We can see that the subtropical anticyclone of Southeastern Japan is strengthened more in CChem run that it is in AChem run, and at this time, accompanied by cold SST in this area. The local air-sea interaction is known to be an important factor in maintaining the subtropical anticyclone in the North Pacific (Seager et al. 2003; Lee et al. 2006). The Western North Pacific subtropical high (WNPSH) gets stronger with a decrease in SST in air-sea coupled models (Song,Zhou 2014). Figures 2e and 2f provide evidence that, with the strengthened monsoon circulation, CChem run yields tropospheric ozone concentrations lower than AChem run over East Asia in August–September.

Interannual variability of tropospheric ozone associated with WNPSH

In the foregoing paragraph, it was suggested that both the WNPSH and monsoon circulation are strengthened when air-sea coupling processes are included in the model simulation, compared to when they are not included. Thus, the East Asian tropospheric simulation is improved in August–September. Because the WNPSH not only affects the climatological East Asian monsoon but greatly impacts the interannual variation of the monsoon (Chang et al. 2000; Sui et al. 2007; Lee et al. 2013; Wang et al. 2013), it is necessary to evaluate the role played by WNPSH in the variability of East Asian ozone concentrations.

An index representing the interannual variability of WNPSH was defined as the geopotential height of 850 hPa, the same as in past studies (Lu,Dong 2001; Xiang et al. 2013). Figure 3 shows the distribution of the standard deviation of the August–September 850 hPa geopotential height, in observation (NCEP), CChem run, and AChem run. The WNPSH index is defined as the normalized time series of the monthly geopotential height anomalies averaged over each rectangle. Although it is oriented slightly to the west, CChem run is highly variable in the Western North Pacific, similar to the observations (Fig. 3a and 3b). On the other hand, in the case of AChem run, no evident variability was observed in the Western North Pacific (Fig. 3c). This implies that the variability in this region is mainly due to the air-sea interaction. Here, the WNPSH index for AChem run was calculated using the same area as CChem run.

The observed East Asian tropospheric ozone dramatically changes according to WNPSH variations (Fig. 4a). The ozone concentrations in the Western North Pacific and the

ISSN: 2056-7537(print), ISSN 2056-7545(online)

northwestern inland of the Korean Peninsula increase when WNPSH is strong. Meanwhile, ozone concentrations decreased in the Asian continental boundary along the Indochina Peninsula, Southeastern China, the Korean Peninsula, and Japan. These regions, where ozone concentrations decrease, are affected by southwesterly and southerly winds associated with WNPSH. It generally coincides with the area where precipitation increases (Fig. 4d). The increase in precipitation weakens photochemical reaction and eliminates ozone precursors in the atmosphere by augmenting clouds and decreasing insolation, ultimately leading to a decrease in ozone. The ozone increase in the Western North Pacific can be explained by a process opposite to this.

In CChem run, ozone concentrations increased in the Western North Pacific and decreased over the Indochina Peninsula, China, and Korea (Fig. 4b). Unlike the observation, the ozone decrease over Japan and its increase in the northwestern Korean Peninsula are not prominent in CChem run. The ozone increase over the Western North Pacific is related to the strengthened WNPSH and the decrease in precipitation, and the ozone decrease in China and Korea should be related to the precipitation increase (Fig. 4e). A remarkable point is that the decrease in ozone concentration in Northern China, where precipitation increases noticeably, is not significant. Such disparity indicates that tropospheric ozone is not simply determined by precipitation or cloud amount. To more precisely simulate ozone concentrations with chemistry-climate models, we need to consider a more elaborate and complicated process.

Regardless of the errors produced by CChem run, its variabilities of the wind, precipitation, and tropospheric ozone due to WNPSH are more accurate than those of AChem run (Fig. 4b and Fig. 4c). The decrease in ozone in observations and in CChem run is not exhibit in AChem run. In fact, AChem run yielded an increase in ozone concentration apparent from the North Pacific to Japan, Korean Peninsula and Eastern China. These errors obtained with AChem run can be expected from the standard deviation of the 850 hPa geopotential height (Fig. 3). In other words, the problem in AChem run is mainly due to the unapparent changes in wind and precipitation associated with the WNPSH variability (Fig 4f), which ultimately results from not including the air-sea interaction (Song,Zhou 2014).

In addition, the CChem run permits to establish a relation between meteorological variables and ozone, which was not easy due to the lack of observation data. Fig. 5a shows the vertical distribution of the averaged (100˚E–120˚E) ozone changes with respect to the WNPSH index. A decrease in ozone is simulated in the entire troposphere over the Indochina region and China (10˚N–40˚N). The decrease in ozone in the mid-latitudes (30˚N–40˚N) is oriented north according to the altitude. Because this vertical structure is similar to the slope of the monsoon front (Fu, Qian 2011), changes in ozone seem to be affected by the monsoon front. This feature can be identified in vertical temperatures and wind changes (Fig. 5b). In other words, a strong temperature rise near 30˚N is expanded towards the upper troposphere along the surface of the front, inclined towards the north. Such characteristics agree with the ozone change shown in 30˚N–45˚N. This figure shows the changes in ozone accompanied by the monsoon front, and implies that the meteorological front is also the chemical front.

SUMMARY

We investigated whether the inclusion of the air-sea coupling processes affect simulations of East Asian ozone concentrations. We used the global atmospheric chemistry model with two

ISSN: 2056-7537(print), ISSN 2056-7545(online)

types of meteorological data produced from the atmospheric model (CAM3/CLM3) and the air-sea coupled model (CCSM3). Anthropogenic emissions and biomass burning emissions were fixed to capture the ozone responses only induced by meteorological changes.

The tropospheric ozone over East Asia during August–September simulated with the meteorological data that incorporated air-sea interaction was in good agreement with the observations. However, when the air-sea interaction is not considered, ozone concentrations were overestimated over China, the Korean Peninsula, and Japan. This can be attributed to the fact that air-sea interactions caused a stronger monsoon circulation and more precipitation; that is still closer to the observations compared to the atmospheric only model. The strengthening of the monsoon by the coupled model led to an intensification of subtropical anticyclones due to the relatively cold SST in the Western North Pacific. Because such characteristics coincide with the results obtained using 17 coupled models and atmospheric models (Song,Zhou 2014), we can say that, to some extent, our results portray a state-of-the–art model.

Not only the average concentrations of tropospheric ozone, the inclusion of air-sea coupling processes also led the chemistry-climate model to well capture the relationship between ozone and WNPSH, one of the causes of interannual variability of the East Asian monsoon. A decrease in ozone concentration was simulated over the China and Korean regions associated with the WNPSH, which was also evident in observations. This is thought to be a consequence of the coupling between the monsoon and atmospheric chemical processes. Interestingly, our model also showed changes in tropospheric ozone associated with the monsoon front. The regions where ozone concentrations decreased are inclined towards the north along the monsoon front. Integration of atmospheric chemistry within weather and climate model and observation will be required to understand chemistry and atmospheric process coupling.

Finally, our results suggest that the air-sea coupling processes need to be considered in order to predict East Asian tropospheric ozone concentrations. This does not only refer to the local effect of SST. In particular, because the SST of the Western North Pacific or the distribution of atmospheric pressure is closely related to ENSO change, ENSO may affect the East Asian tropospheric ozone.

Acknowledgments

This research was supported by the Korea Ministry of Environment (MOE) as “Climate Change Correspondence Program”.

REFERENCES

Bey, I., Jacob, D.J., Yantosca, R.M., Logan, J.A., Field, B.D., Fiore, A.M., Li, Q.B., Liu, H.G.Y., Mickley, L.J. and Schultz, M.G. (2001) Global modeling of tropospheric chemistry with assimilated meteorology: Model description and evaluation. Journal of Geophysical Research-Atmosphere **106**(D19), 23073-23095 doi:10.1029/2001jd000807

Burney, J. and Ramanathan, V. (2014) Recent climate and air pollution impacts on Indian agriculture. Proceedings of the National Academy of Sciences of the United States of America **111**(46), 16319-16324. doi:10.1073/pnas.1317275111

Chang, C.P., Zhang, Y.S. and Li, T. (2000) Interannual and interdecadal variations of the East Asian summer monsoon and tropical Pacific SSTs. Part I: Roles of the subtropical

ISSN: 2056-7537(print), ISSN 2056-7545(online)

ridge. Journal of Climate **13**(24), 4310-4325. doi:10.1175/1520-0442(2000)013<4310:Iaivot>2.0.Co;2

Chatani, S. and Sudo, K. (2011) Influences of the variation in inflow to East Asia on surface ozone over Japan during 1996-2005. Atmospheric Chemistry and Physics **11**(16), 8745-8758. doi:10.5194/acp-11-8745-2011

Doherty, R.M., Stevenson, D.S., Collins, W.J. and Sanderson, M.G. (2005) Influence of convective transport on tropospheric ozone and its precursors in a chemistry-climate model. Atmospheric Chemistry and Physics **5**, 3205-3218

Fu, J.L. and Qian, W.H. (2011) The structure of a typical mei-yu front identified by the equivalent temperature. Atmospheric and Oceanic Science Letters **4**(2), 109-113. doi: 10.1080/16742834.2011.11446913

Han, Z., Sakurai, T., Ueda, H., Carmichael, G.R., Streets, D., Hayami, H., Wang, Z., Holloway, T., Engardt, M., Hozumi, Y., Park, S.U., Kajino, M., Sartelet, K., Fung, C., Bennet, C., Thongboonchoo, N., Tang, Y., Chang, A., Matsuda, K. and Amann, M. (2008) MICS-Asia II: Model intercomparison and evaluation of ozone and relevant species. Atmospheric Environment **42**(15), 3491-3509 doi:10.1016/j.atmosenv.2007.07.031

He, Y.J., Uno, I., Wang, Z.F., Pochanart, P., Li, J. and Akimoto, H. (2008) Significant impact of the East Asia monsoon on ozone seasonal behavior in the boundary layer of Eastern China and the west Pacific region. Atmospheric Chemistry and Physics **8**(24), 7543-7555

Huang, D.Q., Zhu, J., Zhang, Y.C. and Huang, A.N. (2013) Uncertainties on the simulated summer precipitation over Eastern China from the CMIP5 models. Journal of Geophysical Research-Atmosphere **118**(16), 9035-9047. doi:10.1002/jgrd.50695

Jerrett, M., Burnett, R.T., Pope, C.A., Ito, K., Thurston, G., Krewski, D., Shi, Y.L., Calle, E. and Thun, M. (2009) Long-Term Ozone Exposure and Mortality. New England Journal of Medicine **360**(11), 1085-1095. doi:10.1056/NEJMoa0803894

Kurokawa, J., Ohara, T., Uno, I., Hayasaki, M. and Tanimoto, H. (2009) Influence of meteorological variability on interannual variations of springtime boundary layer ozone over Japan during 1981-2005. Atmospheric Chemistry and Physics **9**(17), 6287-6304

Lee, E.J., Yeh, S.W., Jhun, J.G. and Moon, B.K. (2006) Seasonal change in anomalous WNPSH associated with the strong East Asian summer monsoon. Geophysical Research Letters **33**(21). doi:10.1029/2006gl027474

Lee, S.S., Seo, Y.W., Ha, K.J. and Jhun, J.G. (2013) Impact of the western North Pacific subtropical high on the East Asian monsoon precipitation and the Indian Ocean precipitation in the boreal summertime. Asia-Pacific Journal of Atmospheric Sciences **49**(2), 171-182. doi:10.1007/s13143-013-0018-x

Lelieveld, J., Evans, J.S., Fnais, M., Giannadaki, D. and Pozzer, A. (2015) The contribution of outdoor air pollution sources to premature mortality on a global scale. Nature **525**(7569), 367-371. doi:10.1038/nature15371

Lin, M., Holloway, T., Oki, T., Streets, D.G. and Richter, A. (2009) Multi-scale model analysis of boundary layer ozone over East Asia. Atmospheric Chemistry and Physics **9**(10), 3277-3301

Lu, R.Y. and Dong, B.W. (2001) Westward extension of North Pacific subtropical high in summer. Journal of Meteorological Society of Japan **79**(6), 1229-1241. doi:DOI 10.2151/jmsj.79.1229

Park, R.J., Jacob, D.J., Field, B.D., Yantosca, R.M. and Chin, M. (2004) Natural and transboundary pollution influences on sulfate-nitrate-ammonium aerosols in the United

ISSN: 2056-7537(print), ISSN 2056-7545(online)

States: Implications for policy. Journal Geophysical Research-Atmosphere **109**(D15). doi:10.1029/2003jd004473

Parrish, D.D., Law, K.S., Staehelin, J., Derwent, R., Cooper, O.R., Tanimoto, H., Volz-Thomas, A., Gilge, S., Scheel, H.E., Steinbacher, M. and Chan, E. (2013) Lower tropospheric ozone at northern midlatitudes: Changing seasonal cycle. Geophysical Research Letters **40**(8), 1631-1636. doi:10.1002/grl.50303

Seager, R., Murtugudde, R., Naik, N., Clement, A., Gordon, N. and Miller, J. (2003) Air-sea interaction and the seasonal cycle of the subtropical anticyclones. Journal of Climate **16**(12), 1948-1966. doi:Doi 10.1175/1520-0442(2003)016<1948:Aiatsc>2.0.Co;2

Shindell, D., Faluvegi, G., Lacis, A., Hansen, J., Ruedy, R. and Aguilar, E. (2006) Role of tropospheric ozone increases in 20th-century climate change. Journal of Geophysical Research-Atmosphere **111**(D8). doi:10.1029/2005jd006348

Song, F.F. and Zhou, T.J. (2014) The Climatology and Interannual Variability of East Asian Summer Monsoon in CMIP5 Coupled Models: Does Air-Sea Coupling Improve the Simulations? Journal of Climate **27**(23), 8761-8777. doi:10.1175/Jcli-D-14-00396.1

Sui, C.H., Chung, P.H. and Li, T. (2007) Interannual and interdecadal variability of the summertime western North Pacific subtropical high. Geophysical Research Letters **34**(11). doi:10.1029/2006gl029204

Tanimoto, H., Ohara, T. and Uno, I. (2009) Asian anthropogenic emissions and decadal trends in springtime tropospheric ozone over Japan: 1998-2007. Geophysical Research Letters **36**. doi:10.1029/2009gl041382

Wang, B., Ding, Q.H., Fu, X.H., Kang, I.S., Jin, K., Shukla, J. and Doblas-Reyes, F. (2005) Fundamental challenge in simulation and prediction of summer monsoon rainfall. Geophysical Research Letters **32**(15). doi:10.1029/2005gl022734

Wang, B., Xiang, B.Q. and Lee, J.Y. (2013) Subtropical High predictability establishes a promising way for monsoon and tropical storm predictions. Proceedings of the National Academy of Sciences of the United States of America **110**(8), 2718-2722. doi:10.1073/pnas.1214626110

Wang, T., Wei, X.L., Ding, A.J., Poon, C.N., Lam, K.S., Li, Y.S., Chan, L.Y. and Anson, M. (2009) Increasing surface ozone concentrations in the background atmosphere of Southern China, 1994-2007. Atmospheric Chemistry and Physics **9**(16), 6217-6227

Xiang, B.Q., Wang, B., Yu, W.D. and Xu, S.B. (2013) How can anomalous western North Pacific Subtropical High intensify in late summer? Geophysical Research Letters **40**(10), 2349-2354. doi:10.1002/grl.50431

Ziemke, J.R., Chandra, S., Duncan, B.N., Froidevaux, L., Bhartia, P.K., Levelt, P.F. and Waters, J.W. (2006) Tropospheric ozone determined from aura OMI and MLS: Evaluation of measurements and comparison with the Global Modeling Initiative's Chemical Transport Model. Journal of Geophysical Research-Atmosphere **111**(D19). doi:10.1029/2006jd007089

Ziemke, J.R., Chandra, S., Labow, G.J., Bhartia, P.K., Froidevaux, L. and Witte, J.C. (2011) A global climatology of tropospheric and stratospheric ozone derived from Aura OMI and MLS measurements. Atmospheric Chemistry and Physics **11**(17), 9237-9251. doi:10.5194/acp-11-9237-2011

ISSN: 2056-7537(print), ISSN 2056-7545(online)

APPENDIX

Table 1. Summary of Experiments

Exp. Name	CCSM3 component set	Air-sea coupled processes in meteorological variables to drive the GEOS-Chem	Period
AChem	CAM3/CLM3 forced observed SST	Yes	40 years (1971–2010)
CChem	Fully coupled	No	45 years (total CESM run 280 y)

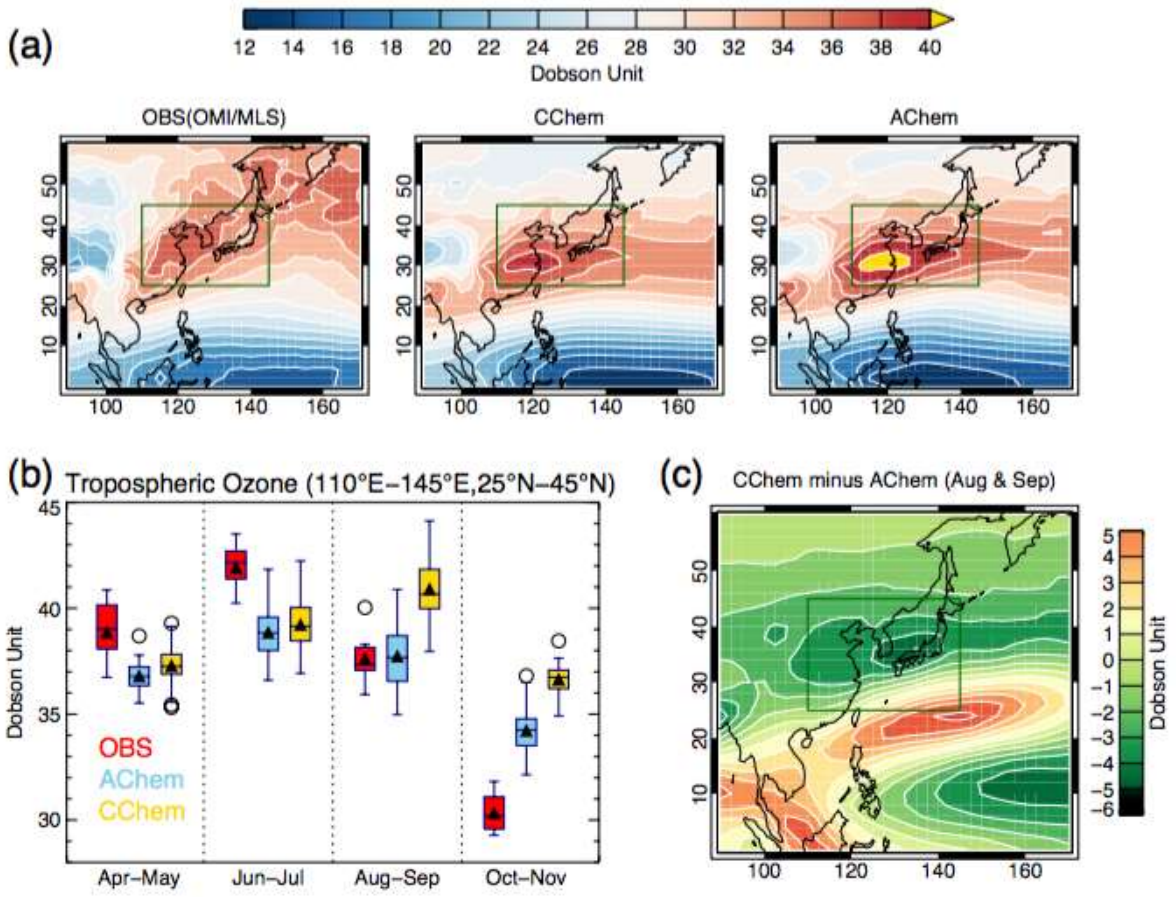

Figure 1. (a) Climatological distributions of the tropospheric ozone (Dobson Unit) from observation (2005–2014), CChem run (45-year simulation), and AChem run (1971–2010). (b) Boxplots for the two consecutive monthly averaged tropospheric ozone over East Asia denoted by the green rectangles (110°E–

ISSN: 2056-7537(print), ISSN 2056-7545(online)

145°E, 25°N–45°N) in (a) from OMI/MLS (red), CChem (blue), and AChem (yellow). The heights of the filled boxes indicate the interquartile range (IQR; 25–75% range) whereas the line and triangle inside indicates the median and mean, respectively. The vertical whiskers extent to the values corresponding to the 1.5 times the IQR of the box. Open circles beyond the whiskers indicate outliers. (c) Difference in tropospheric ozone between CChem run and AChem run.

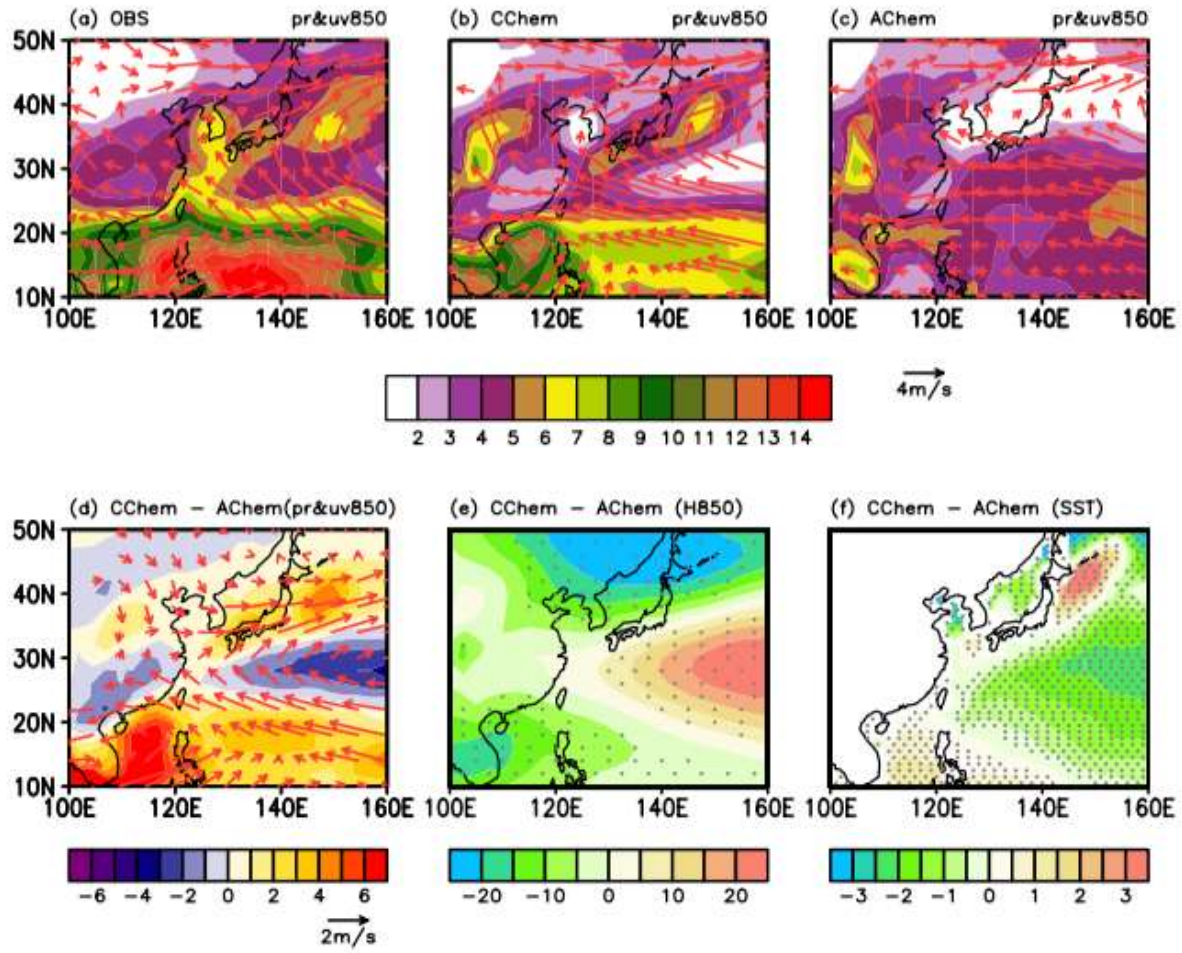

Figure 2. Averaged precipitation (shading, mm/day) and 850hPa wind vector during August–September for (a) observation (CMAP and NCEP reanalysis), (b) CChem, and (c) AChem run. Differences between CChem run and AChem run from (d) precipitation (shading, mm/day) and 850hPa wind vector, (e) 850 hPa geopotential height (m), and (f) sea surface temperature (°C).

ISSN: 2056-7537(print), ISSN 2056-7545(online)

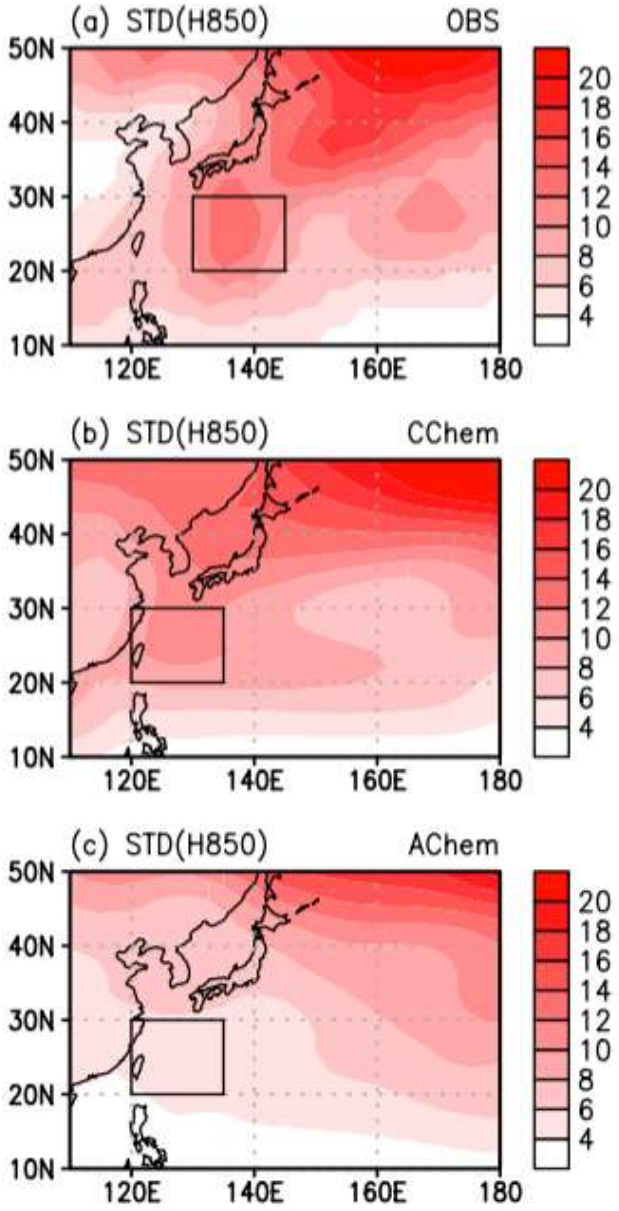

Figure 3. The standard deviation (m) of 850 hPa geopotential heights from (a) NCEP reanalysis, (b) CChem run, and (c) AChem run. The boxes represent the area for calculation of WNPSH index.

ISSN: 2056-7537(print), ISSN 2056-7545(online)

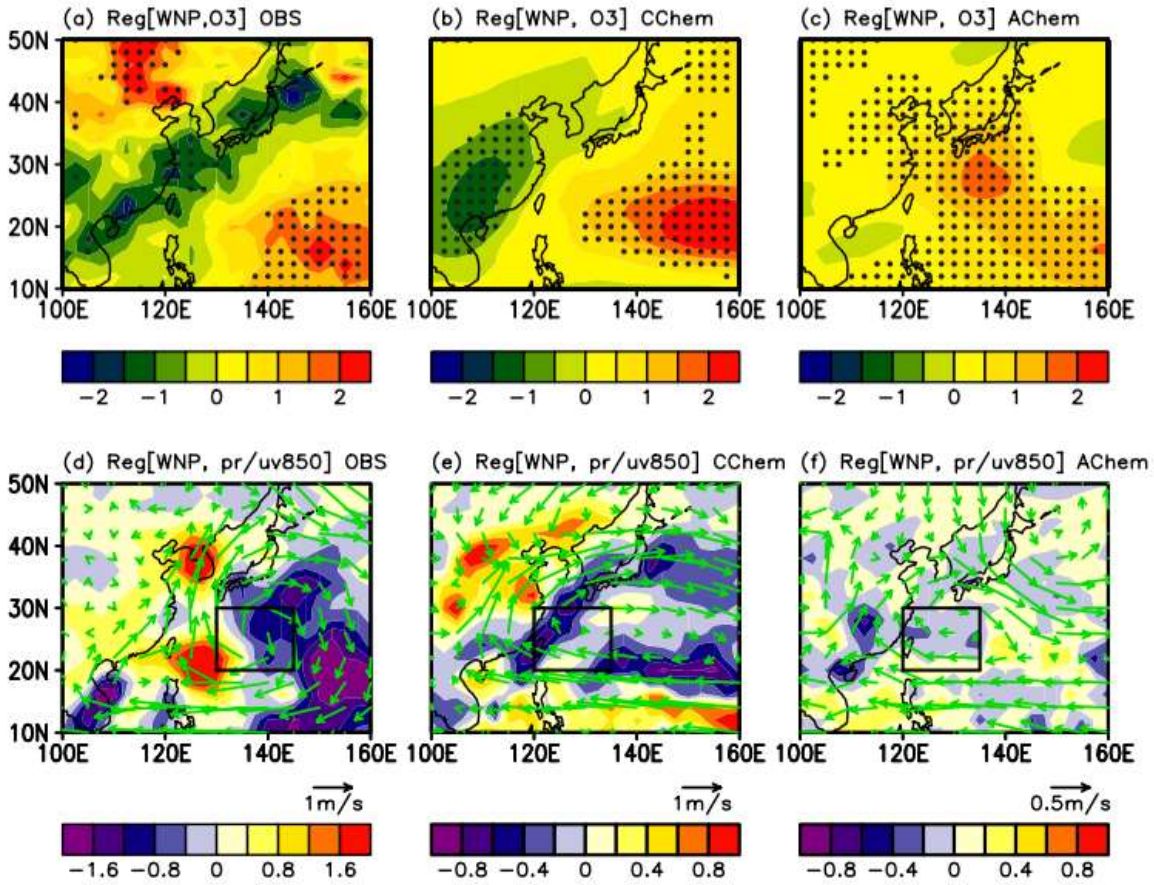

Figure 4. The regressed tropospheric ozone (DU) against the normalized WNPSH index for (a) observation, (b) CChem run, and (c) AChem run. Dotted areas denote the statistically significant at 90% confidence level by t-test. (d–f) are the same as (a–c), except the regressed precipitation and 850 hPa wind vectors. Boxes are the same in the Fig. 3.

ISSN: 2056-7537(print), ISSN 2056-7545(online)

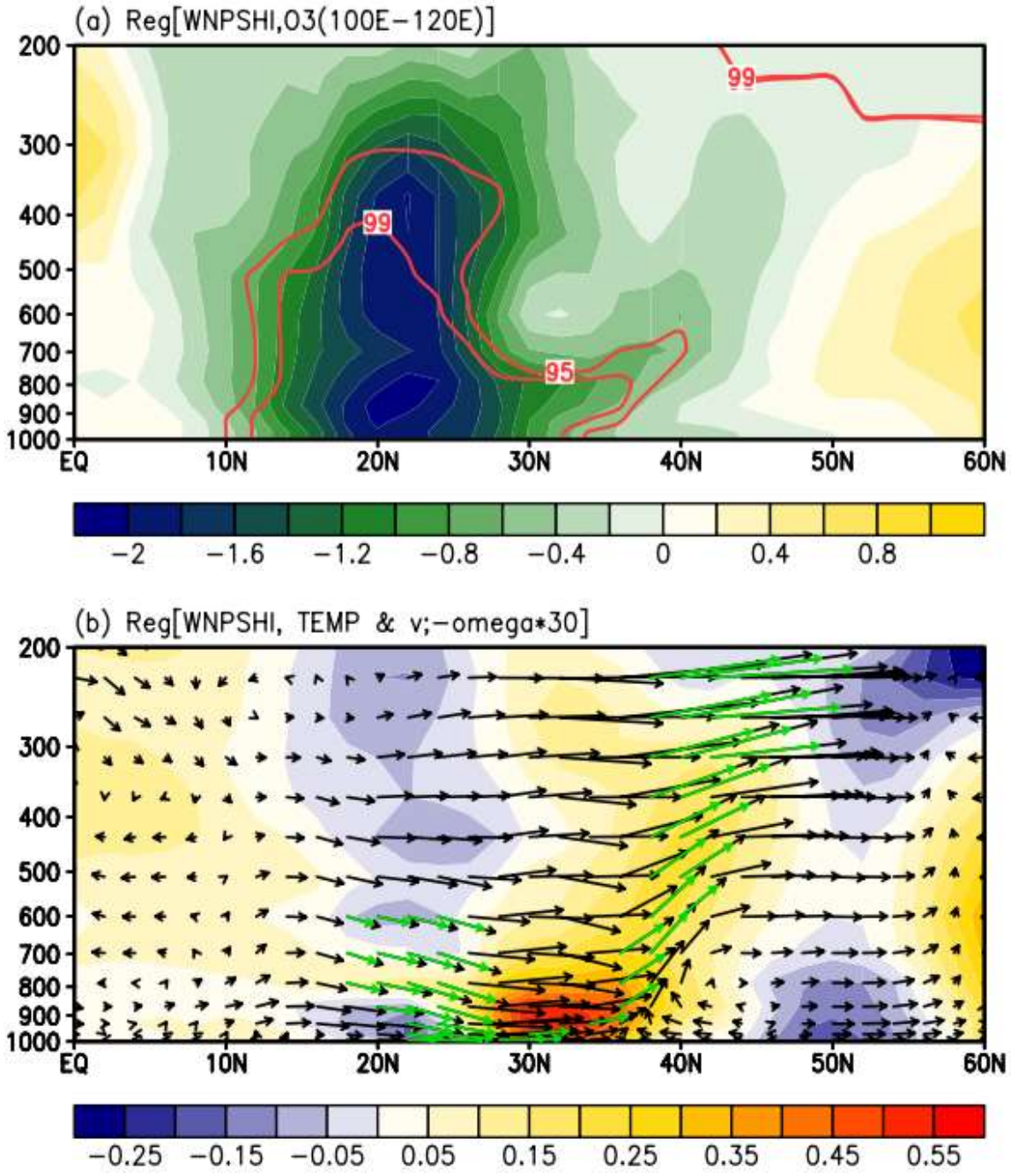

Figure 5. The vertical cross section in regressed (a) ozone (ppbv) and (b) temperature (℃) and winds against the normalized WNPSH index along 100˚E–120˚E. Note that omega is multiplied by –30 to exaggerate the variations. Green arrows indicate the statistically significant at 95% confidence level by t-test.

ISSN: 2056-7537(print), ISSN 2056-7545(online)